Telecommun Syst (2015) 59:5–23
DOI 10.1007/s11235-014-9883-6

Exploiting diversity of usage to enhance user equipment energy efficiency in LTE networks

Tuan Ta · John S. Baras

Published online: 10 December 2014

Abstract Energy efficiency is widely recognized as an important factor for future cellular networks. For mobile devices, energy efficiency leads to extended battery life. Existing works consider battery to be equally important for all users at all time. We recognize that the value of a device's battery depends on the user's target usage. In particular, we introduce the notions of *valueless* and *valued battery*, as being the available battery when the user does or does not have access to a power source, respectively. We argue that user experience only depends on valued battery. We propose a cooperative system to help raise the overall amount of valued battery in the network. Our system makes use of device-to-device communications underlaying LTE to create cooperative relay links between users. Users who expect to have a large amount of valueless battery help relay traffic for users with a small amount of valued battery. We develop our system as a proximity service for future LTE releases. We propose a framework to study utility functions to evaluate the value of battery. We show that with appropriate utility functions, a set of thresholding cooperative rules ensure network performance improvement. We illustrate this improvement through simulation. Our simulator source code is made available to the public.

Keywords D2D · Energy efficiency · Proximity service · LTE · Resource sharing

T. Ta (✉) · J. S. Baras
Department of Electrical and Computer Engineering, Institute for Systems Research, University of Maryland, College Park, USA
e-mail: tta@umd.edu

J. S. Baras
e-mail: baras@umd.edu

1 Introduction

Smartphones have become an essential part of our everyday life. They have been outselling PC since 2010 [1]. The number of smartphones as well as the amount of data they generate keep increasing at a dramatic pace [2]. However, one of the biggest problems limiting the usefulness of smartphones is their short battery life. Battery technology lags far behind the demand for smartphone usage. The energy consumption on smartphones has been broken down into components [3,4]. It is shown that network communications and the display are the two biggest contributors, significantly higher than other components such as memory and processor. As cloud computing becomes the de facto platform for intensive computational tasks, the ability to always stay connected is even more important.

Energy efficient designs for wireless communications have been widely recognized as an important topic. The traditional goal of energy efficient designs is to maximize the number of bits transmitted per energy unit. Solutions are proposed across layers of wireless networks. On network planning level, the impact of cell size as well as mixed cell deployment on energy consumption of the devices have been studied [5,6]. On application layer, energy-efficient video coding schemes have been proposed [7]. On network layer, energy-aware routing protocols have been developed for distributed wireless networks [8]. On MAC layer, energy efficiency has been incorporated in resource allocation algorithms [9,10]. On PHY layer, adaptive MIMO modulation orders according to channel condition have been proposed [11]. In addition, cross-layer solutions have been developed. Route selection and MIMO constellation size are jointly considered to enhance energy efficiency of wireless sensor networks in [12].

By maximizing the number of bits transmitted per unit energy, existing work make an implicit assumption that energy, in absolute quantity (Joules), is worth the same for all users at any time instant. We, on the other hand, realize that smartphone battery does not always have the same value for the users. A straightforward argument is that a user will not value his battery as much when he has a high battery bar compared to when he has a low battery bar. We take this argument one step further. The user will not value his battery much, even if he has a low battery bar, if he is only a few minutes from home. Therefore the value of the battery to a user involves both the absolute amount as well as the user's target usage. In particular, we introduce the notion of *valued battery*, defined as the battery of the smartphone when the user is active and does not have access to a power source. Similarly, *valueless battery* is defined as the battery of the smartphone when the user has access to a power source. We argue that the user's experience depends only on his valued battery. Smartphone users often are quite concerned when they are on the road, and their (valued) battery drops low. However, the abundant number of occasions when they are at home and their (valueless) battery is high often go unnoticed.

In realistic cellular networks, users have varied amount of remaining battery. When the state of the battery (with respect to access to a charging source) is taken into account, this variation becomes even larger. We call this phenomenon *diversity of usage*. It is intuitive that the network as a whole will benefit from converting valueless battery into valued battery. Since we are still far away from efficient long-distance wireless energy transfer [13], a more practical approach to "sharing" battery among users needs to be developed.

Recent advancements in device-to-device (D2D) communications underlaying cellular networks provide us with a perfect opportunity to create such a practical approach to energy sharing. D2D communications, as the name suggests, are the practices of creating direct links between cellular devices. The original goals of D2D communications are to offload data from the congested cellular networks, as well as to provide opportunities for direct advertisements and alternative communication mediums for public safety operations during catastrophes. We envision a new usage for D2D communications. Most of the power in wireless transmissions is spent to overcome distance-dependent path loss. Since D2D connections are local, their path loss is much smaller than that of cellular links. Therefore, for the same quality of service, D2D connections consume less power.

In [14], we propose a cooperative system, the "Battery Deposit Service" (BDS), which makes use of D2D communications underlaying LTE, to provide energy sharing in the form of load sharing. Our system allows users with high battery level to help relay traffic of users with low battery level through a D2D connection. Since the direct link costs much less power than the cellular link, the usage time of users with low battery level is prolonged. The cooperative selection criteria are designed carefully such that the amount of energy the helpers expend does not reduce their usage time to below their target usage. Thus they only spend valueless battery. As a result, our system takes advantage of diversity of usage to raise the overall amount of valued battery in the network. In this work, we provide a more thorough description of our system and introduce several important improvements.

There are four main technical areas that need to be addressed in developing our system. The first area is system architecture. This includes invoking appropriate entities within the evolved packet system (EPS) and developing signaling protocols for UEs to request and provide help. The second area is studying the utility of battery for the users to design cooperative criteria such that the overall network performance is improved. The third area is management of user incentive. Intuitively, every user can benefit from the system at some point in time. However, the benefit for the helpers is not immediate, therefore there need to be mechanisms to incentivize users and prevent selfish behaviors. The fourth area is accurate estimation of user target usage. Machine learning algorithms, assisted by a vast amount of user data, are continuing to produce better prediction [15]. In this work, we will assume that we receive accurate user target usages and address the first three areas.

1.1 Related work

We introduced the idea of our system in [14]. In that work, we used two widely accepted channel models, IST WINNER II model [16] and UMTS model [17] to show that the power consumption in a D2D connection can be 3 to 4 orders of magnitude less than that of a cellular connection. Therefore, when a user (the *helper*) relays uplink traffic for another user (the *helpee*), the helper carries the cost of that communication session for the helpee. Effectively, the helper "transfers" some of his energy to the helpee. Equivalently, the helper and helpee can be thought of as "depositing" energy into and "withdrawing" energy out of the network. The diversity of usage in the network ensures that with high probability, the helper will run low on battery at some other time and receive help. The depositing and withdrawing analogies are appropriate because they signify that the helping relationship needs not be immediate or reciprocal. The helper can receive help from a different user at a different time. These analogies give rise to the name of our system, the "Battery Deposit Service" (BDS).

We created a simulator (written in MATLAB) [18] to evaluate the performance of BDS under some realistic channel, traffic, and mobility models. In [14], we formulated the cooperative decisions based only on the amount of available battery of the users. As discussed above, the target usage also

plays an important role. In this work we will address both values in the design of cooperative rules. In [14] we assume that the users are altruistic. In this work we will address mechanisms to manage user incentive.

D2D communications can operate on both unlicensed (out-of-band) and licensed spectrum (in-band). Because of the popularity of technologies such as Wifi and bluetooth, out-of-band D2D communications have traditionally been the main focus, drawing a large body of literature. For instance, in [19,20], Wifi D2D connections are utilized to enhance energy efficiency in the context of content dissemination applications. In LTE, however, in-band D2D communication is the preferred method by 3GPP. The main advantage of having D2D links on licensed spectrum is that interference can be managed. This leads to predictable performance of the D2D links. Moreover, in-band D2D connection setup can be transparent to the users. Since each device context has already been established with the cellular network, a secure D2D connection can be set up automatically (as opposed to manual pairing in Wifi and bluetooth). Since guaranteeing QoS and low-latency connection setup are a crucial features of our cooperative relay system, using in-band D2D communications is the nature choice for BDS.

Prior work on in-band D2D have been mainly concerned with interference management and resource allocation [21–23]. If done properly, they enable D2D connections to exist concurrently with regular cellular connections at "no cost". In fact, through measurements on a wide spectrum range (20 MHz to 6 GHz) from 4 locations in Germany, Netherlands, California, [24] observes that on average, 50 % of the spectrum in is never used, 26 % is only partially used. In particular, the cellular uplink bands (GSM and UMTS) are mostly idle because the uplink signals are very weak to be detected even with high-end spectrum analyzers. For BDS, it means that the D2D relay links can coexist with other cellular links with minimal impact on system throughput. In this work we will assume the eNodeB knows the optimal way to allocate resource for D2D links and focus on the energy sharing problem.

In order to utilize D2D communications in a systematic way, 3GPP created a work item named "Study on Proximity-based Services" (ProSe) for release 12 [25]. To enable ProSe, changes need to be made on both network architecture, non-access stratum (NAS) and access stratum (AS) protocols. In [26,27], additional logical entities are proposed in the evolved packet core (EPC) to manage D2D-capable devices and ProSe applications. A new type of data bearer between D2D UEs, D2D bearer, is also proposed. Additional control signaling to manage D2D bearers is considered. We use these suggestions in developing our system architecture.

Even though not studied in cellular contexts, energy harvesting networks share some similarities with our utility analysis. In an energy harvesting network, nodes rely on energy from some natural sources to operate. Since the amount of energy and the harvesting instants are usually random, the value of energy for a node changes over time. This characteristic is similar to our observation that the value of smartphone battery is dependent upon both the amount and the time (with respect to the user target usage). Prior research on energy harvesting networks have proposed scheduling algorithms for nodes to adapt to their harvesting process [28]. The goal is to control the energy expenditure to reduce the probability of exhausting available resource, thus disrupting network operations. In contrast to these work, in cellular context, the smartphones do not control the user usage. Therefore the research questions are fundamentally different. Usage, instead of being the output, is given as the input to BDS (in the form of some probabilistic model). The decision space is to find the best cooperative rules (instants and duration), given that model and the amount of available battery. In addition, nodes in energy harvesting networks are all under the designer's control. In our case, the users need to be incentivized to cooperate.

Incentive schemes in wireless networks have been studied for over a decade. Most existing works aim to create an incentive system for nodes in a mobile ad-hoc network to forward packets from their neighbors [29–32]. Three main incentive mechanisms have been proposed: reputation, Tit-for-Tat, and currency. In a reputation system, each time a node cooperates truthfully, its reputation in the network is increased. Highly reputable nodes receive good service from others. Nodes with low reputation may be denied from participating. In a Tit-for-Tat system, a pair of nodes take turn to perform services for each other in multiple rounds. Each node therefore has incentive to act honestly in fear of not getting service from the other in future rounds. In a currency system, nodes buy and sell services. The price of the service is determined by the market. The currency can either be real dollars or virtual.

Since in our case, we want a node to be able to interact with many other nodes, Tit-for-Tat is not suitable. Reputation works well in distributed systems, but the performance is hard to be predicted exactly. Currency fits our needs the best. It gives us an *exact* method to keep track of the transactions in the networks. The network plays a major role here, as a bank/moderator. In currency system without a central control entity, accounting is a major challenge. For virtual currency systems, the amount of virtual money is normally attached to each packet, protected by cryptographic measures. Not only does it incur processing overhead, cryptographic key distribution and management also poses as a big problem. Fake virtual money as well as double spending need to be taken into account as well. Some notable implementations of distributed virtual currency include Bitcoin [33], Nuglets [29], and WhoPay [34].

1.2 Summary of contribution

Our contribution in this work is to identify new cooperative opportunities in cellular networks, by taking advantage of diversity of usage, to prolong battery life on mobile devices. We develop a proximity service as defined by 3GPP for UEs to participate in cooperation.

1. System architecture: We identify responsible entities in the EPS and develop signaling for service request and setup.
2. System cooperative rules: We propose a general framework to study utility of resource and apply that framework to our system. We show that by using appropriate utility thresholds as cooperative rules, the system performance can be guaranteed to improve.
3. User incentive: We consider currency systems that provide incentive for users to participate faithfully.

1.3 Outline of paper

BDS system architecture is described in Sect. 2. In Sect. 3 we introduce a general framework to study utility of resource and apply it to BDS. We discuss user incentive in Sect. 4. We analyze BDS performance through simulation in Sect. 5. We conclude and discuss future work in Sect. 6.

2 System architecture

We envision battery deposit service (BDS) as a proximity service (ProSe) in future releases of LTE. It is clear that to support ProSe, there need to be additional entities in EPC as well as new NAS and AS protocols [26,27]. We assume that the mobility management entity (MME) has an additional function, *ProSe management* (PSM), which manages D2D-related device capabilities, identifier allocation, connection establishment, mobility tracking, etc. We also assume there is an *application server* (AppSer) that communicates with the policy and charging rules function (PCRF) to enforce policy compliance for ProSe applications. The AppSer can make request to the PSM in the MME to setup D2D connections for ProSe applications.

We discussed security implications of BDS in [14]. We showed that BDS does not incur any more security risk than what can already be obtained by an eavesdropper. Moreover, in [14], we introduced the basic flow of BDS . In this work, we make use of the additional entities PSM and AppSer to propose a detail signaling procedure to set up a BDS cooperative relay session. This signaling procedure is illustrated in Fig. 1. We consider an example where the helpee UE1 is associated with eNodeB1. The PSM, which manages UE1's D2D connections, knows that UE1's potential D2D peers are connected to eNodeB1 and eNodeB2. In this example, UE2, which is connected to eNodeB2, is selected to be the helper for UE1. The PSM notifies the serving gateway (S-GW) to update UE1's data path, which changes from UE1 ↔ eNodeB1 ↔ S-GW to UE1 ↔ UE2 ↔ eNodeB2 ↔ S-GW.

The overall procedure can be divided into three smaller subroutines: discovery, D2D bearer establishment, and BDS cooperative relay.

Discovery

1. The helpee UE1, under some conditions, decides to request for BDS service. It sends `BDSInitSerReq` to the PSM inside the MME.
2. The PSM forwards the request, together with UE1 ID, to the AppSer in the form of `BDSSerReq`.
3. The AppSer checks UE1 policy (by contacting the PCRF) to decide if UE1 is allowed to use BDS service.
4. Once confirmed, it sends a response `BDSSerResp` to the PSM.
5. The PSM sends `BDSDiscoveryConfig` message with the helpee ID (UE1) to eNodeB1 and eNodeB2.
6. eNodeB1 and eNodeB2 agree on a time/frequency resource for a BDS discovery signal and send this information to UE1 (the discoverer) through a `RRCConn Reconfig` message. (6a) This time/frequency resource is also sent to all BDS-enabled UEs within their cells (the listeners) through `RRCConnReconfig` messages. We envision that there can be a group control message format to make this process more efficient.
7. UE1 sends the discovery signal `BDSDiscovery`.
8. The subset of listeners who were able to hear UE1's `BDSDiscovery` send their replies, in the form of `BDSReply` messages, to the PSM. The PSM forwards them to the AppSer.
9. `BDSReply` messages contain information required by the AppSer to select the optimal helper for UE1. Some possible decision rules include
   - Max-battery: in `BDSReply`, the UEs include their remaining battery levels. The AppSer selects the UE with highest remaining battery to help.
   - Proximity: in `BDSReply`, the UEs include the received signal strength of UE1's `BDSDiscovery` signal. The AppSer selects the UE with highest received signal strength (i.e. it is closest to UE1).
   - Currency: to ensure fairness and manage user incentive, a currency system is set up by the AppSer. The selection rule in this system is discussed in Sect. 4.

Let UE2 be the chosen helper. At the end of the discovery phase, the helper/helpee association is determined.

D2D Bearer Establishment

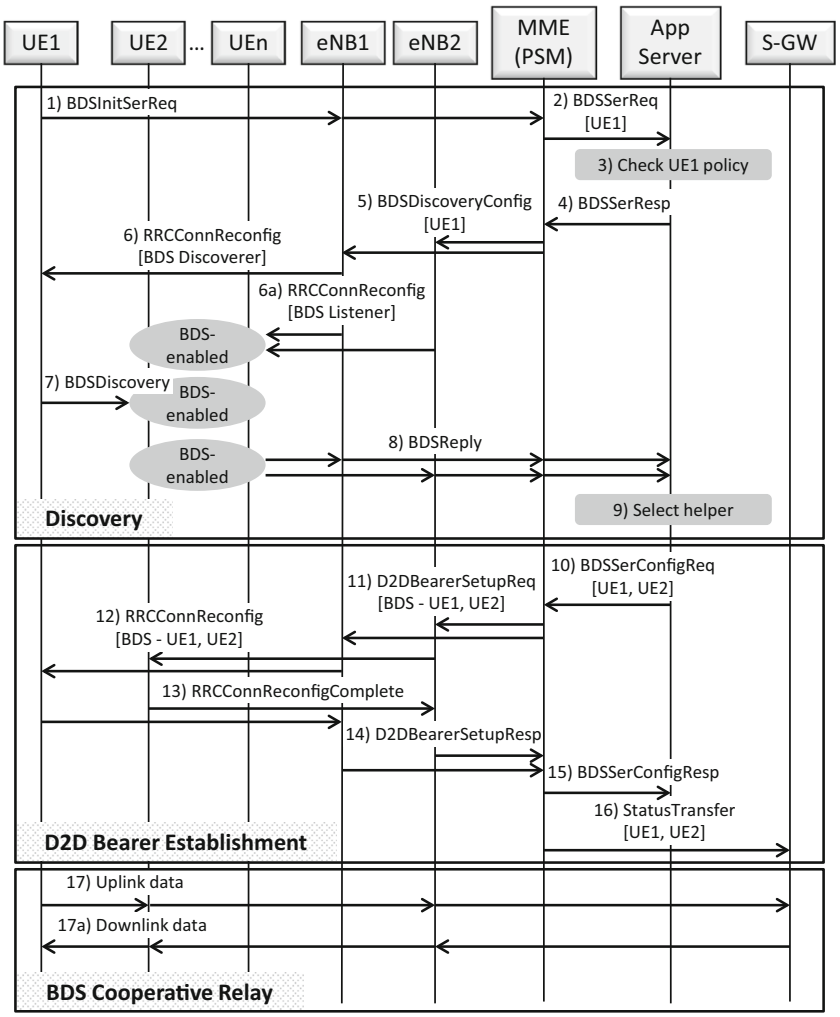

Fig. 1 Signaling flow for establishment of a BDS cooperative relay session. UE1 is the helpee, UE2 is the selected helper

10. The AppSer sends a request, `BDSSerConfigReq`, to the PSM to create a D2D connection for BDS with UE1 and UE2 IDs.
11. The PSM sends `D2DBearerSetupReq` to request eNodeB1 and eNodeB2 to allocate resource for a D2D connection between UE1 and UE2. The QoS of the D2D connection can also be included.
12. eNodeB1 and eNodeB2 send `RRCConnReconfig` commands to UE1 and UE2 to inform them of the D2D resource.
13. UE1 and UE2 confirm that they are ready to use the allocated resource for D2D communications by sending `RRCConnReconfigComplete`.
14. eNodeB1 and eNodeB2 inform the PSM that the D2D bearer setup is complete by sending `D2DBearerSetupResp`.
15. The PSM informs the AppSer that the BDS service configuration is complete by sending `BDSSerConfigResp`.
16. The PSM informs the S-GW to update UE1's status by sending `StatusTransfer`. Future IP data packets to UE1 should be routed through eNodeB2.

At the end of the D2D bearer establishment, UE2 is ready to relay UE1's data traffic.

BDS Cooperative Relay

17. During the cooperative session, UE1's data path is updated to UE1 $\leftrightarrow$ UE2 $\leftrightarrow$ eNodeB2 $\leftrightarrow$ S-GW.

3 Cooperative rules

BDS system architecture allows the UEs to request for service whenever they want. The potential helpers can also choose when they want to respond to `BDSDiscovery`. Intuitively, we want the UEs to only request for service when they cannot satisfy their own usage demand. At the same time, the UEs should only respond to help requests if doing so does not hurt their ability to meet their target usage. In this section, by studying battery utility for the UEs, we design cooperative rules to enforce those behaviors.

BDS belongs to a general class of systems in which the resource for each user is generated and/or consumed

according to some random processes. Because of the randomness, there are possibilities that the available resource of some users cannot meet their consumption requests. At the same time, other users may have unused resource. Therefore the users can benefit from resource transferring among themselves. We start with a general framework to study resource utility and apply that utility analysis to design cooperative rules. We then study BDS as a specific case.

3.1 General utility analysis framework

Our framework considers a system in which the users consume a limited amount of resource over time. The system has two main characteristics

- The resource consumption or the resource generation, or both, are random
- Resource can be transferred between users according to a transfer graph

The goal of the users is to satisfy the resource consumption, given the resource generation process. We use the notion of a target usage duration to study user utility. The target usage duration is the period until the next arrival of resource. Given the current amount of available resource, the utility for a user is related to his ability to meet this usage.

We first define our terminology. Next, we discuss user performance in term of utility. Using utility, we consider conditions in which cooperation is beneficial for participants. Finally, we consider two broad categories of systems and two specific utility functions that are appropriate to those categories.

3.1.1 Terminology

Let us consider a system with multiple users, indexed by $i = 1, 2, \ldots$ At each instance, the state of user i consists of the following quantities

- B_i: the amount of remaining resource, $B_i \geq 0$.
- T_i: the target usage duration, $T_i \geq 0$.
- L_i: the parameter for the resource consumption process.

From those instantaneous state variables, the following future quantities can be derived

- $\zeta_{L_i}(\tau)$: the amount of resource consumed for usage duration τ, given the parameter L_i. $\zeta_{L_i}(\tau)$ is a random process, $\forall L, \forall \tau \geq 0 : \zeta_L(\tau) \geq 0$.
- T_{Oi}: the duration until the resource runs out (*time until outage*). T_{Oi} is a random variable which satisfies $\zeta_{L_i}(T_{Oi}) = B_i$. $T_{Oi} \geq 0$.
- T_{Vi}: the amount of valued usage time. Valued usage time is smaller of the time until outage and the target usage. T_{Vi} is a random variable defined as $T_{Vi} = \min(T_i, T_{Oi})$. $T_{Vi} \geq 0$.

Subsequently, we will drop the subscript i when it is clear from the context that we are talking about a general user.

3.1.2 User utility

Since the users have limited resource, there is a possibility that they do not meet their target usage. The likelihood of this possibility depends on future resource consumption. In this framework, we will consider users to receive maximum utility if their target usage is met. In the case where the users' target usage is not met, their utility depends on the specific type of resource and application. We investigate two broad categories of applications in subsequent sections. First, we discuss some properties of a general utility function.

We consider users with higher utility to be in better states. For the same target usage, more resource gives better utility. Similarly, with the same level of remaining resource, the user with shorter target usage has higher utility. Therefore, the utility function has to be monotonically non-decreasing in B and monotonically non-increasing in T. In other words,

$$u(B_1, T, L) \geq u(B_2, T, L) \quad \text{for } B_1 \geq B_2 \tag{1}$$

$$u(B, T_1, L) \geq u(B, T_2, L) \quad \text{for } T_1 \leq T_2 \tag{2}$$

Through cooperation, resource can be transferred between users, which alters the time until outage for both parties. The novelty in our approach is the consideration of the target usage time T. In Fig. 2 we show an example of a utility function for visualization. The resource B and target usage duration T are normalized to some B^* and T^*. The values of B^* and T^* are not important for the current discussion. Here we are only interested in the shape of the utility surface. A user i with low resource (B_i small), but requires usage for only a short duration (T_i small) can have higher utility than a user j with more resource (B_j large), but also requires usage for a long period (T_j large). As a result, user i can potentially provide more help than user j. This way we utilize cooperative opportunities that otherwise were not available in previous frameworks that only consider the amount of available resource B.

Any utility function needs to have the following properties

P1. Ease of computing: The users need to monitor their utility frequently, therefore the utility calculation should be very fast.

P2. Ease of deriving cooperation rules: The purpose of the utility function is to determine cooperation rules for the users. Therefore, a good utility function simplifies these rules.

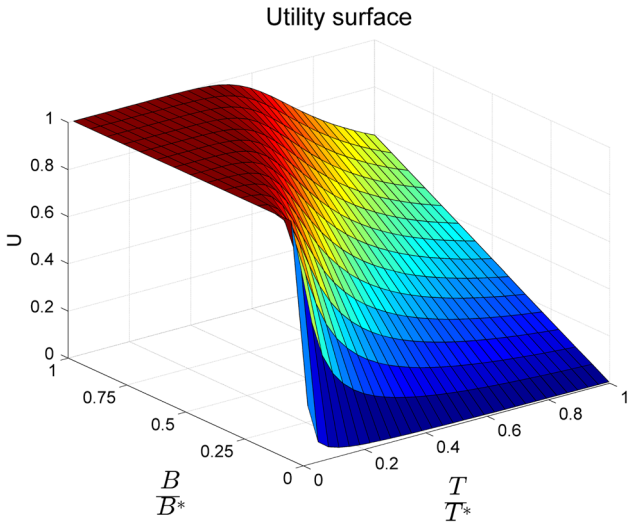

Fig. 2 A sample utility surface. The resource B and target usage duration T are normalized. Following a curve with constant target usage time, the utility function increases with B—property (1). Following a curve with constant resource, the utility function decreases with T—property (2)

3.1.3 Beneficial cooperation

Let us consider a cooperative session in which user i is the helpee and user j is the helper. The cooperative session has duration T_c. During this session, the helper transfers an amount of resource, $\Delta B_{ji} \geq 0$, to the helpee. The resource transferring loss is denoted δ_{ji}. Without loss of generality, the transferring loss is associated with the helpee. Table 1 illustrates the condition of the helper and helpee before and after cooperation.

Definition 1 A cooperative session is *beneficial* if the total utility with cooperation is no less than the total utility without cooperation.

$$\begin{aligned} &u_i(B_i - \zeta_{L_i}(T_c) + \Delta B_{ji} - \delta_{ji}, T_i - T_c, L_i) \\ &\quad + u_j(B_j - \zeta_{L_j}(T_c) - \Delta B_{ji}, T_j - T_c, L_j) \\ &\geq u_i(B_i - \zeta_{L_i}(T_c), T_i - T_c, L_i) \\ &\quad + u_j(B_j - \zeta_{L_j}(T_c), T_j - T_c, L_j). \end{aligned} \tag{3}$$

Equivalently, the cooperative utility gain of the helpee is, in magnitude, at least equal to the cooperative utility loss of the helper.

$$\begin{aligned} &u_i(B_i - \zeta_{L_i}(T_c) + \Delta B_{ji} - \delta_{ji}, T_i - T_c, L_i) \\ &\quad - u_i(B_i - \zeta_{L_i}(T_c), T_i - T_c, L_i) \\ &\geq u_j(B_j - \zeta_{L_j}(T_c), T_j - T_c, L_j) \\ &\quad - u_j(B_j - \zeta_{L_j}(T_c) - \Delta B_{ji}, T_j - T_c, L_j). \end{aligned} \tag{4}$$

If the system is designed such that only beneficial cooperative sessions are allowed, the overall utility of the network will increase in cooperation.

Lemma 1 *A necessary condition for a cooperative session to be beneficial is that the resource transferring loss is no greater than the amount of resource transferred by the helper.*

$$\delta_{ji} \leq \Delta B_{ji}. \tag{5}$$

Proof See Appendix 1.

In a beneficial cooperative session, if the transferring loss is positive, the total amount of resource consumed is greater than that of the non-cooperative case. However, by definition, the total utility is improved. This is achieved because the helper and the helpee are on different operating points with respect to their utilities. For the case where the cooperative session length is much smaller than the target usage time of both users, $T_c \ll T_i, T_j$, from (4) we see that the helpee must be operating on a "steeper" resource-slope than the helper. In other words,

$$\frac{\partial}{\partial B} u_i(B_i, T_i, L_i) > \frac{\partial}{\partial B} u_j(B_j, T_j, L_j). \tag{6}$$

As a result, a larger change in resource for the helper results in a smaller change in utility. This knowledge can be used to design cooperative rules.

3.1.4 Two categories of systems

In this section we discuss two broad categories of systems and the appropriate utility function for each category.

C1. The users only concern with whether or not their task is done (all or nothing). If a user's target usage is satisfied, he receives utility 1, otherwise he receives utility 0.

Table 1 Target usage duration and remaining resource of the helper and helpee before and after cooperation

		Helpee (i)		Helper (j)	
		Target usage	Remaining resource	Target usage	Remaining resource
Before		T_i	B_i	T_j	B_j
After	Non-coop	$T_i - T_c$	$B_i - \zeta_{L_i}(T_c)$	$T_j - T_c$	$B_j - \zeta_{L_j}(T_c)$
	Coop		$B_i - \zeta_{L_i}(T_c)$ $+\Delta B_{ji} - \delta_{ji}$		$B_j - \zeta_{L_j}(T_c)$ $-\Delta B_{ji}$

C2. The users concern with the amount of usage they receive, up to the target usage. Users whose target usage is met receive maximum utility. Whereas users whose target usage is not met receive utility proportional to their usage time. Another way to think about this category is that if the users do not meet their target usage, they incur a cost proportional to the amount of time they come short. Users who meet their target usage have zero cost.

We consider two utility functions, one for each category of systems, and their computational complexity. As discussed in Sect. 3.1.2, it is desirable that a utility function is easy to compute.

3.1.4.1 Category C1: probability of survival For users who receive utility 1 when their usage is satisfied, and utility 0 otherwise, the *probability of survival*, $\mathbb{P}[T_O > T]$, is their expected utility. First we define *probability of outage*, the probability that a user (with state B, T, L) will run out of resource before his target usage

$$P_O = \mathbb{P}[T_O \leq T] = \mathbb{P}[\zeta_L(T) \geq B]. \tag{7}$$

The utility function is thus

$$u_1(B, T, L) = 1 - P_O. \tag{8}$$

3.1.4.2 Category C2: Expected valued usage time For this category, the expected amount of valued usage time as a fraction of the target usage time, $\mathbb{E}[T_V]/T$, is a good performance metric. The reason for normalization can be better understood by an example. Let us consider user A who wants to use his phone for 4 h without charging. If his expected valued usage time is 3 h, his utility will be 0.75. User B with a 2-h target usage but only 1 h of expected valued time has utility 0.5. Notice that in both cases, the user needs 1 extra hour to meet his target usage. The fact that user A has higher utility illustrates that 1 h is not worth as much for him as it is for user B. This is justified considering that user A has a larger amount of target usage compared to user B.

The expected usage time is

$$\begin{aligned}\mathbb{E}[T_V] &= \mathbb{E}[\min(T_O, T)] \\ &= \int_0^T \tau f_{T_O}(\tau) d\tau + \int_T^\infty T f_{T_O}(\tau) d\tau \\ &= \mathbb{E}[T_O] - \int_T^\infty (\tau - T) f_{T_O}(\tau) d\tau \qquad (9) \\ &= T - \int_0^T (T - \tau) f_{T_O}(\tau) d\tau. \qquad (10)\end{aligned}$$

The utility function for this category of users is defined as

$$u_2(B, T, L) = \frac{\mathbb{E}[T_V]}{T}. \tag{11}$$

Here $f_{T_O}(\cdot)$ denotes the PDF of the time until outage, the CDF of which is given by the consumption process

$$\mathbb{P}[T_O \leq \tau] = \mathbb{P}[\zeta_L(\tau) \geq B]. \tag{12}$$

3.1.4.3 Computation of $u_1(\cdot)$ and $u_2(\cdot)$ It can be easily verified that both $u_1(\cdot)$ and $u_2(\cdot)$ satisfy (1) and (2). Moreover, we can see that both utility functions depend crucially on the time until outage T_O, which in turn depends on the consumption process $\zeta_L(\cdot)$. Therefore, the computational speed of these utility functions also depends on the underlying consumption process. While there are no closed-form expressions for $u_1(\cdot)$ and $u_2(\cdot)$ for a general consumption process, we discuss a few cases where efficient approximations can be used to speed up the computation.

First we consider the two extremes. If the user's resource is very high compared to his target usage, i.e. the distribution of T_O increases much slower than linear before the target usage, then he is very unlikely to go into outage: $P_O \approx 0$. In this case the target usage dominates in calculation of the valued usage time (10) can be used to approximate $\mathbb{E}[T_V]$.

If $(T - \tau) f_{T_O}(\tau) \approx 0$ for $\tau \leq T$:

$$u_1 = 1 - P_O \approx 1 \tag{13}$$

$$u_2 = \frac{\mathbb{E}[T_V]}{T} \approx 1. \tag{14}$$

Similarly, if the user's resource is very low compared to his target usage, i.e. the distribution of T_O decreases much faster than linear after the target usage, then he is very likely to go into outage: $P_O \approx 1$. Whereas the time until outage dominates in the calculation of the valued usage time. (9) can be used to approximate $\mathbb{E}[T_V]$.

If $(\tau - T) f_{T_O}(\tau) \approx 0$ for $\tau \geq T$:

$$u_1 = 1 - P_O \approx 0 \tag{15}$$

$$u_2 = \frac{\mathbb{E}[T_V]}{T} \approx \frac{\mathbb{E}[T_O]}{T}. \tag{16}$$

Outside of the two extremes, a special case where the utility functions can be efficiently approximated is when the consumption process is Gaussian. In other words, $\zeta_L(\tau) \sim \mathcal{N}(\mu_L(\tau), \sigma_L^2(\tau))$. From (12), the CDF of time until outage is

$$\mathbb{P}[T_O \leq \tau] = \mathbb{P}[\zeta_L(\tau) \geq B] = \Phi\left(\frac{\mu_L(\tau) - B}{\sigma_L(\tau)}\right). \tag{17}$$

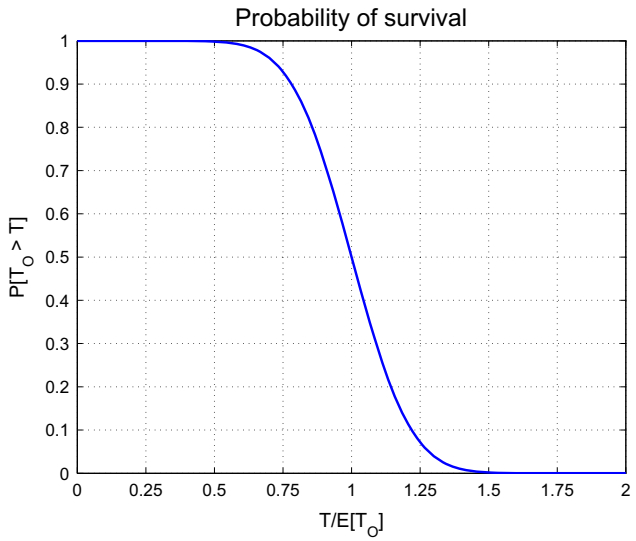

(a) C1 - Probability of survival (18)

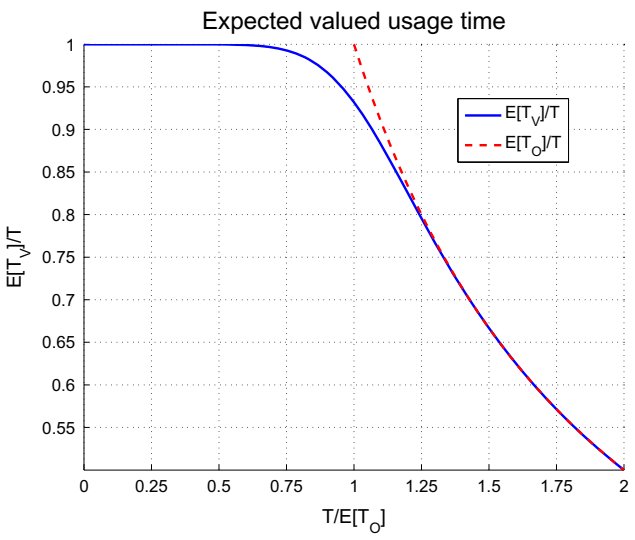

(b) C2 - Expected valued usage time (21)

Fig. 3 Utility as functions of target usage time for user categories C1 and C2. The amount of available resource is fixed. Both utility functions show two clear extremes. **a** C1: probability of survival (18). **b** C2: expected valued usage time (21)

Where $\Phi(\cdot)$ denotes the standard Normal CDF. The probability of survival is simply

$$u_1 = 1 - \Phi\left(\frac{\mu_L(T) - B}{\sigma_L(T)}\right) = \Phi\left(\frac{B - \mu_L(T)}{\sigma_L(T)}\right). \tag{18}$$

If the mean of the consumption process scales linearly with the duration, i.e. $\mu_L(\tau) = \lambda_L \tau$, then

$$\mathbb{P}[T_O \leq \tau] = \Phi\left(\frac{\tau - B/\lambda_L}{\sigma_L(\tau)/\lambda_L}\right). \tag{19}$$

By approximating τ in $\sigma_L(\tau)$ by B/λ_L, we get $\sigma_L(\tau)/\lambda_L \approx \sigma_L(B)$. Denote $\mu_L(B) = B/\lambda_L$, (19) becomes

$$\mathbb{P}[T_O \leq \tau] \approx \Phi\left(\frac{\tau - \mu_L(B)}{\sigma_L(B)}\right). \tag{20}$$

As a result, the time until outage can be approximated as having a Gaussian distribution $\mathcal{N}(\mu_L(B), \sigma_L^2(B))$. The calculation of expected valued usage time according to (10) becomes (see Appendix 1)

$$\mathbb{E}[T_V] \approx T - (T - \mu_L(B))\Phi\left(\frac{T - \mu_L(B)}{\sigma_L(B)}\right) + \frac{\sigma_L(B)}{\sqrt{2\pi}}\left(e^{-\frac{\mu_L(B)^2}{2\sigma_L(B)^2}} - e^{-\frac{(T-\mu_L(B))^2}{2\sigma_L(B)^2}}\right). \tag{21}$$

With the closed forms (18) and (21), the utility functions can be computed efficiently.

Figure 3 illustrates the two utility functions when the consumption process is Gaussian. The utility functions are plotted against the target usage duration T while fixing the amount of available resource B. The mean usage duration, $\mathbb{E}[T_O]$, is used as the reference. For both utility functions, we can see clearly the two discussed extremes. At their lower (higher) extreme, u_1 is very close to 1 (0), whereas u_2 is very close to 1 ($\mathbb{E}[T_O]/T$).

3.2 Battery deposit service

In this section, we apply the previous framework for mobile UEs in a BDS system. The resource here is the communication energy budget of the UEs. When we talk about the battery of a user, we refer to the communication energy budget. As discussed in [14], uplink transmission power dominates other communication-related components in term of energy consumption. Therefore we will only consider the uplink transmission power in the theoretical analysis. Other factors such as idle circuit power and downlink reception power are considered in simulation. As seen in Sect. 3.1, the main component of the system is the battery consumption process $\zeta_L(t)$.

3.2.1 Battery consumption process $\zeta_L(t)$

First, we describe the uplink power consumption of UEs in LTE networks. We then introduce the user's data traffic model. These two components make up the battery consumption process.

3.2.1.1 LTE uplink power control The battery consumption for the UEs follows LTE uplink power control [35,36]. The uplink transmission power in dB is

$$P_{\mathrm{UL}} = \underbrace{P_0 + \alpha \mathrm{PL}}_{\text{open-loop}} + \underbrace{\Delta_{\mathrm{TF}} + f(\Delta_{\mathrm{TPC}})}_{\text{dynamic offset}} + 10\log_{10}(M). \quad (22)$$

P_{UL} consists of two components. The first component depends on the state of the UE with respect to the eNodeB. This component is further comprised of two subcomponents: a basic open-loop operating point and a dynamic offset. The second component depends on the amount of uplink data, which is realized in term of M, the number of allocated resource blocks. A resource block (RB) is the basic unit of time-frequency resource allocation in LTE. It consists of 12 OFDM subcarriers (for the total bandwidth of 180 kHz with 15 kHz subcarrier spacing) over one slot (0.5 ms).

P_0 is a semi-static nominal power level set by the eNodeB. αPL is the path loss compensation component, where α controls the degree of compensation. PL is derived from the downlink Reference Signal Received Power. It includes shadowing but not fast fading. The dynamic control of UE uplink transmit power is designed to be an offset from the base operating point. This offset depends on two factors: the allowed modulation and coding scheme (TF stands for Transport Format) and a UE-specific transmitter power control (TPC) command.

While P_0, PL as well as the dynamic control of P_{UL} change over time, a complete model of these quantities depends on many factors such as user movement, traffic load within the cell, eNodeB strategy etc. In this work, we use instantaneous values of these quantities in the formulation of the consumption process. Each time a UE computes its utility, it updates these quantities.

The battery consumption process is

$$\zeta_L(t) = 10^{\frac{P_0+\alpha\mathrm{PL}+\mathrm{DO}}{10}} M(t) = \rho_0 M(t), \quad (23)$$

where DO is the dynamic offset. $M(t)$ is the data arrival process, in unit of resource blocks.

3.2.1.2 Traffic model We model $M(t)$ as a Poisson burst process with rate λ. Each burst size is modeled as a geometric random variable with parameter ν. Poisson processes are commonly used in traffic modeling because they capture well the aggregate traffic caused by a large number of sources (e.g. applications in a smartphone). Similar models were used by Nokia and Renesas Mobile Europe in their recent 3GPP contributions [37,38].

Let us denote the Poisson arrival process $N(t)$, and the size of each arrival M (in resource blocks). M is assumed i.i.d. between different arrivals.

We have, for $n \geq 0$

$$\mathbb{P}[N(t) = n] = \frac{(\lambda t)^n}{n!} e^{-\lambda t}, \quad (24)$$

and for $m \geq 1$

$$\mathbb{P}[M = m] = (1-\nu)^{m-1}\nu. \quad (25)$$

From (23),

$$\zeta_L(t) = \rho_0 M(t) = \rho_0 \sum_{i=1}^{N(t)} M_i \quad (26)$$

$\zeta_L(t)$ is a Poisson burst process with rate λ and takes values as integer multiplies of ρ_0. As a result, we can discretize the battery using ρ_0 as a basic unit.

As seen in Sect. 3.1, computing the distribution of the time until outage, $\mathbb{P}[T_O \leq t]$, is the most important task for the utility methods of BDS. In the following section, we discuss in detail this computation.

3.2.2 Distribution of time until outage T_O

In this section we describe two methods to compute exactly the CDF of T_O and an approximation for quick calculation.

3.2.2.1 Stochastic analysis Recall that for a UE with state (B, T, L), $\mathbb{P}[T_O \leq t] = \mathbb{P}[\zeta_L(t) \geq B]$. From (26), with the available battery B written as multiples of ρ_0, we can write the compliment of the CDF of T_O as

$$\begin{aligned}\mathbb{P}[T_O \geq t] &= \mathbb{P}[\zeta_L(t) \leq B] \\ &= \sum_{n=0}^{\infty} \mathbb{P}[N(t) = n]\mathbb{P}\left[\sum_{i=1}^{n} M_i \leq B\right] \\ &= \sum_{n=0}^{B} \mathbb{P}[N(t) = n]\mathbb{P}\left[\sum_{i=1}^{n} M_i \leq B\right]. \end{aligned} \quad (27)$$

Since M_i are i.i.d. geometric(ν) random variables, we can think of $\sum_{i=1}^{n} M_i$ as the total number of Bernoulli trials before the first n successes. Each Bernoulli trial has success probability ν. Since each $M_i \geq 1$, $\mathbb{P}\left[\sum_{i=1}^{n} M_i \leq B\right] = 0$ for $n > B$. For $n \leq B$, we have

$$\begin{aligned}&\mathbb{P}\left[\sum_{i=1}^{n} M_i = B\right] \\ &= \underbrace{\binom{B-1}{n-1}(1-\nu)^{B-n}\nu^{n-1}}_{\text{first } n-1 \text{ successes in } B-1 \text{ trials}} \underbrace{\nu}_{\text{last success}}. \end{aligned} \quad (28)$$

This is the probability mass function of a negative binomial random variable NB(n, ν). The CMF of which is

$$\mathbb{P}\left[\sum_{i=1}^{n} M_i \leq B\right] = \sum_{k=n}^{B} \binom{k-1}{n-1} (1-\nu)^{k-n}\nu^n \tag{29}$$

$$= \sum_{j=n}^{B} \binom{B}{j} (1-\nu)^{B-j}\nu^j \tag{30}$$

$$= I_\nu(n, B-n+1), \tag{31}$$

(29) can be interpreted as while fixing the number of success n we sum over the cases when the total number of trials is at most B. (30) can be interpreted as while fixing the total number of trials B, we sum over the cases when the number of successes are at least n. $I_\nu(\cdot,\cdot)$ is the regularized incomplete beta function, whose expression is given in (30) [39].

Plugging (31) into (27) we have

$$\mathbb{P}[T_O \leq t] = 1 - \mathbb{P}[T_O \geq t]$$

$$= 1 - \sum_{n=0}^{B} \frac{(\lambda t)^n}{n!} e^{-\lambda t} I_\nu(n, B-n+1). \tag{32}$$

3.2.2.2 Markovian analysis We can see that $\zeta_L(t)$ is a jump process, therefore it can be analyzed under Markovian theory. The state space is discrete, with each state being the number of remaining battery units. As a result, we have a homogeneous continuous time Markov Chain as shown in Fig. 4.

Let the state variable be $X \in \mathbb{N}$, the transition probability is defined as

$$p_{ij}(t) = \mathbb{P}[X(t) = j | X(0) = i], \qquad i, j \in \mathbb{N}. \tag{33}$$

From (28) and (31), we have

$$\begin{cases} p_{00}(t) = 1, & \\ p_{ii}(t) = e^{-\lambda t}, & i > 0 \\ p_{ij}(t) = \sum_{n=1}^{i-j} \frac{(\lambda t)^n}{n!} e^{-\lambda t} \binom{i-j-1}{n-1} (1-\nu)^{i-j-n}\nu^n, & i > j > 0 \\ p_{i0}(t) = \sum_{n=1}^{\infty} \frac{(\lambda t)^n}{n!} e^{-\lambda t} \left(1 - I_\nu(n, i-n)\right), & i > 0 \\ p_{ij}(t) = 0, & i < j \end{cases} \tag{34}$$

Define the *local characteristics* for any state i

$$q_i = \lim_{h\to 0} \frac{1 - p_{ii}(h)}{h}, \tag{35}$$

and for any pair of states $i \neq j$

$$q_{ij} = \lim_{h\to 0} \frac{p_{ij}(h)}{h}. \tag{36}$$

For the Poisson arrival process, as time duration $h \to 0$, the probability of having 2 or more arrivals during h vanishes. Therefore we only need to account for $n = 1$ in the third and fourth terms of (34). Taking the limits, we get

$$\begin{cases} q_{0,j} = 0, & \forall j \\ q_i = \lambda, & i > 0 \\ q_{ij} = \lambda(1-\nu)^{i-j-1}\nu, & i > j > 0 \\ q_{i0} = \lambda(1-\nu)^{i-1}, & i > 0 \end{cases} \tag{37}$$

The last equation of (37) is derived by plugging in $n = 1$ in the fourth equation of (34) and using the following properties of the regularized incomplete beta function [39].

$$1 - I_\nu(1, i-1) = I_{1-\nu}(i-1, 1)$$

$$= \nu \sum_{j=i-1}^{\infty} (1-\nu)^j$$

$$= (1-\nu)^{i-1} \tag{38}$$

Let $q_{ii} = -q_i$, the matrix $\mathbf{A} = \{q_{ij}\}$ is called the *infinitesimal generator* of the Markov Chain. It takes the form $\mathbf{A} = -\lambda\mathbf{\Lambda}$, where

$$\mathbf{\Lambda} = \begin{bmatrix} 0 & 0 & 0 & 0 & 0 & \\ -1 & 1 & 0 & 0 & 0 & \\ -(1-\nu) & -\nu & 1 & 0 & 0 & \cdots \\ -(1-\nu)^2 & -(1-\nu)\nu & -\nu & 1 & 0 & \\ -(1-\nu)^3 & -(1-\nu)^2\nu & -(1-\nu)\nu & -\nu & 1 & \\ & & \vdots & & & \ddots \end{bmatrix} \tag{39}$$

Denote the transition matrix $\mathbf{P}(t) = \{p_{ij}(t)\}$. From the definition of the local characteristics q_{ij} in (35) and (36), we have

$$\mathbf{A} = \lim_{h\to 0} \frac{\mathbf{P}(h) - \mathbf{P}(0)}{h}, \tag{40}$$

where $\mathbf{P}(0) = \mathbf{I}$. Since this Markov Chain is homogeneous

$$\frac{\mathbf{P}(t+h) - \mathbf{P}(t)}{h} = \mathbf{P}(t)\frac{\mathbf{P}(h) - \mathbf{I}}{h} = \frac{\mathbf{P}(h) - \mathbf{I}}{h}\mathbf{P}(t). \tag{41}$$

Therefore

$$\frac{d}{dt}\mathbf{P}(t) = \mathbf{P}(t)\mathbf{A} = \mathbf{A}\mathbf{P}(t) \tag{42}$$

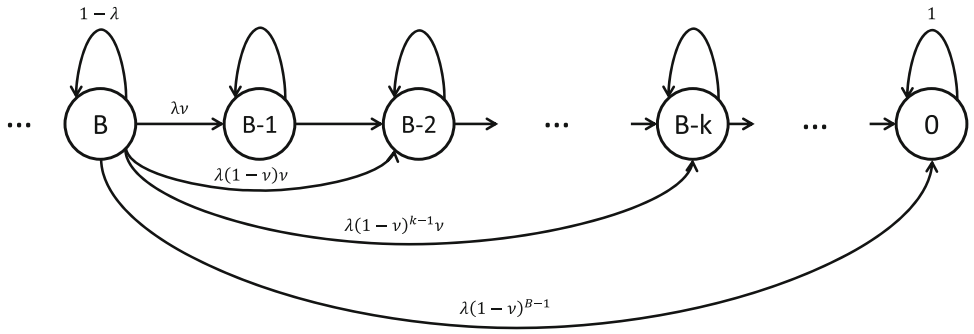

Fig. 4 Continuous time Markov chain for remaining battery states

(42) is referred to as the Kolmogorov's differential system [40], the solution to which is

$$\mathbf{P}(t) = e^{t\mathbf{A}} = \sum_{n=0}^{\infty} \frac{(t\mathbf{A})^n}{n!} \tag{43}$$

Since $X = 0$ is an absorbing state, the CDF of the time until outage, $\mathbb{P}[T_O \leq t]$, is the probability that the UE enters state $X = 0$ at or before t, starting with B battery units at time 0. It can obtained from $\mathbf{P}(t)$ as follows

$$\mathbb{P}[T_O \leq t] = \mathbb{P}[X(t) = 0 | X(0) = B] = p_{B0}(t). \tag{44}$$

3.2.2.3 Gaussian approximation In this section we follow the analysis in Sect. 3.1.4.3 for the case in which the consumption process is Gaussian. First we establish that $\zeta_L(t)$ can indeed be approximated as a Gaussian random process. Recall from (26) that $\zeta_L(t) = \rho_0 \sum_{i=1}^{N(t)} M_i$. Since M_i are i.i.d., if $N(t)$ is sufficiently large, we can use the Central Limit Theorem to approximate $\zeta_L(t)$ as a Gaussian random process $\mathcal{N}\left(\mu_L(t), \sigma_L^2(t)\right)$. We proceed to find the mean and variance of this process.

Recall that each M_i is distributed as a geometric random variable M with parameter ν. We have

$$\begin{aligned} \mathbb{E}[M] &= \frac{1}{\nu} \\ \text{Var}[M] &= \frac{1-\nu}{\nu^2}. \end{aligned} \tag{45}$$

From the law of total expectation,

$$\begin{aligned} \mu_L(t) &= \mathbb{E}\left[\mathbb{E}\left[\rho_0 \sum_{i=1}^{N(t)} M_i \middle| N(t)\right]\right] \\ &= \rho_0 \mathbb{E}[N(t)]\mathbb{E}[M] \\ &= \rho_0 \frac{\lambda t}{\nu} \end{aligned} \tag{46}$$

From the law of total variance,

$$\begin{aligned} \sigma_L^2(t) &= \mathbb{E}\left[\text{Var}\left[\rho_0 \sum_{i=1}^{N(t)} M_i \middle| N(t)\right]\right] \\ &\quad + \text{Var}\left[\mathbb{E}\left[\rho_0 \sum_{i=1}^{N(t)} M_i \middle| N(t)\right]\right] \\ &= \rho_0^2 \mathbb{E}[N(t)]\text{Var}[M] + \rho_0^2 \text{Var}[N(t)]\mathbb{E}[M]^2 \\ &= \rho_0^2 \lambda t \frac{1-\nu}{\nu^2} + \rho_0^2 \lambda t \frac{1}{\nu^2} \\ &= \rho_0^2 \lambda t \frac{2-\nu}{\nu^2} \end{aligned} \tag{47}$$

From (17), by using the remaining battery B as multiple of the battery unit ρ_0, we have

$$\mathbb{P}[T_O \leq t] = \Phi\left(\frac{\frac{\lambda t}{\nu} - B}{\sqrt{\lambda t \frac{2-\nu}{\nu^2}}}\right). \tag{48}$$

Using the approximation in (20), we replace the value of t on the denominator of (48) with $\frac{B\nu}{\lambda}$. (48) becomes

$$\begin{aligned} \mathbb{P}[T_O \leq t] &\approx \Phi\left(\frac{t - \frac{B\nu}{\lambda}}{\frac{\nu}{\lambda}\sqrt{\lambda \frac{B\nu}{\lambda} \frac{2-\nu}{\nu^2}}}\right) \\ &= \Phi\left(\frac{t - \frac{B\nu}{\lambda}}{\sqrt{\frac{B\nu(2-\nu)}{\lambda^2}}}\right). \end{aligned} \tag{49}$$

Therefore, for a given amount of battery B, the time until outage T_O can be approximated as a Gaussian random variable $\mathcal{N}(\mu_{T_O}, \sigma_{T_O}^2)$, with

$$\mu_{T_O} = \frac{B\nu}{\lambda}, \qquad \sigma_{T_O}^2 = \frac{B\nu(2-\nu)}{\lambda^2}. \tag{50}$$

We compare the CDF of the time until outage T_O calculated by stochastic analysis (32), Markovian analysis (44), Gaussian approximation (50), and Monte Carlo simulation in

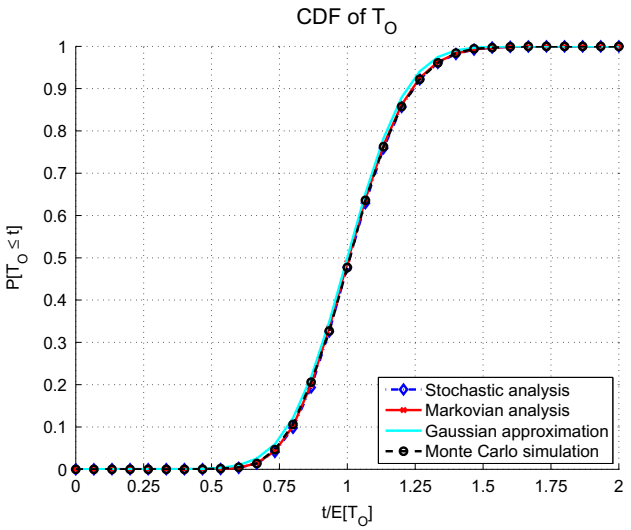

Fig. 5 CDF of time until outage T_O calculated by stochastic analysis (32), Markovian analysis (44), Gaussian approximation (50), and Monte Carlo simulation. The time duration t is plotted with reference to the mean usage duration $\mathbb{E}[T_O]$

Fig. 5. It can be clearly seen that the stochastic and Markovian analyses agree with the Monte Carlo simulation. The Gaussian approximation is very close to this precise distribution.

3.2.3 Beneficial cooperation

In this section we study the conditions which a helpee i and a helper j engaging in a beneficial cooperative session (Definition 1) must satisfy. Let the duration of this cooperative session be T_c. The helpee's consumption process parameter L_i comprises of the battery unit $\rho_{0,i}$ and the helpee's data arrival characteristics λ_i, ν_i. $\rho_{0,i}$ depends on the helpee's uplink power control parameters, of which the main component is the path loss PL_i. Similarly, the helper's consumption process parameter L_j comprises of $\rho_{0,j}, \lambda_j$, and ν_j. Because the helper relays the helpee's data during the cooperative session, the consumption process parameter L_{ij} of the cooperative session consists of the D2D path loss PL_{ij} (thus battery unit $\rho_{0,ij}$) and the helpee's data arrival characteristics λ_i, ν_i. Here we make an implicit assumption that the transmission power in D2D mode is proportional to the path loss between the devices. If 3GPP chooses to use constant D2D transmission power then L_{ij} only depends on λ_i, ν_i.

During the cooperative session, the helpee transmits its data through the D2D link. Its battery consumption is

$$\Delta B_i = \rho_{0,ij} \sum_{k=1}^{N_i(T_c)} M_{i,k} \tag{51}$$

During the cooperative session, the helper transmits both of its data and the helpee's data to the eNodeB. The amount of battery consumed by receiving D2D data is very small compared to the uplink transmission, thus can be ignored. The helper's battery consumption is

$$\Delta B_j = \rho_{0,j} \left(\sum_{k=1}^{N_i(T_c)} M_{i,k} + \sum_{l=1}^{N_j(T_c)} M_{j,l} \right) \tag{52}$$

Refer to Table 1, the amount of battery "transferred" by the helper is

$$\Delta B_{ji} = \rho_{0,j} \sum_{k=1}^{N_i(T_c)} M_{i,k}. \tag{53}$$

The transferring loss at the helpee is

$$\delta_{ji} = (\rho_{0,j} - \rho_{0,i}) \sum_{k=1}^{N_i(T_c)} M_{i,k} + \rho_{0,ij} \sum_{k=1}^{N_i(T_c)} M_{i,k}. \tag{54}$$

According to Lemma 1, to have beneficial cooperation, we need $\delta_{ji} \leq \Delta B_{ji}$. From (53) and (54), this condition is equivalent to

$$\rho_{0,ij} \sum_{k=1}^{N_i(T_c)} M_{i,k} \leq \rho_{0,i} \sum_{k=1}^{N_i(T_c)} M_{i,k}. \tag{55}$$

In other words, the helpee needs to spend less energy in a D2D link than he would in the cellular link. This is typically the case, unless the helpee is very close to the eNodeB. In BDS, we enforce a maximum D2D path loss PL_{D2D} such that only helpers who receive the `BDSDiscovery` signal with received path loss smaller than this value will respond with `BDSReply` (Fig. 1). This threshold essentially limits the range of the D2D connections, keeping them "local". The condition in Lemma 1 can be enforced by only allowing the helpees to request for help when their path loss is greater than PL_{D2D}. More formally, we have

$$\rho_{0,i} \geq \rho_{0,D2D} \geq \rho_{0,ij} \tag{56}$$

where $\rho_{0,D2D}$ is calculated based on PL_{D2D}.

3.2.4 Design of cooperative rules

In BDS, the cooperative duration T_c is kept small so that user mobility does not make the D2D link go out of range. If after T_c, the helper and the helpee still satisfy the beneficial cooperative conditions, they can request the eNodeB to extend the cooperative duration to another T_c. This will reduce the amount of signaling as the helpee does not need to go through

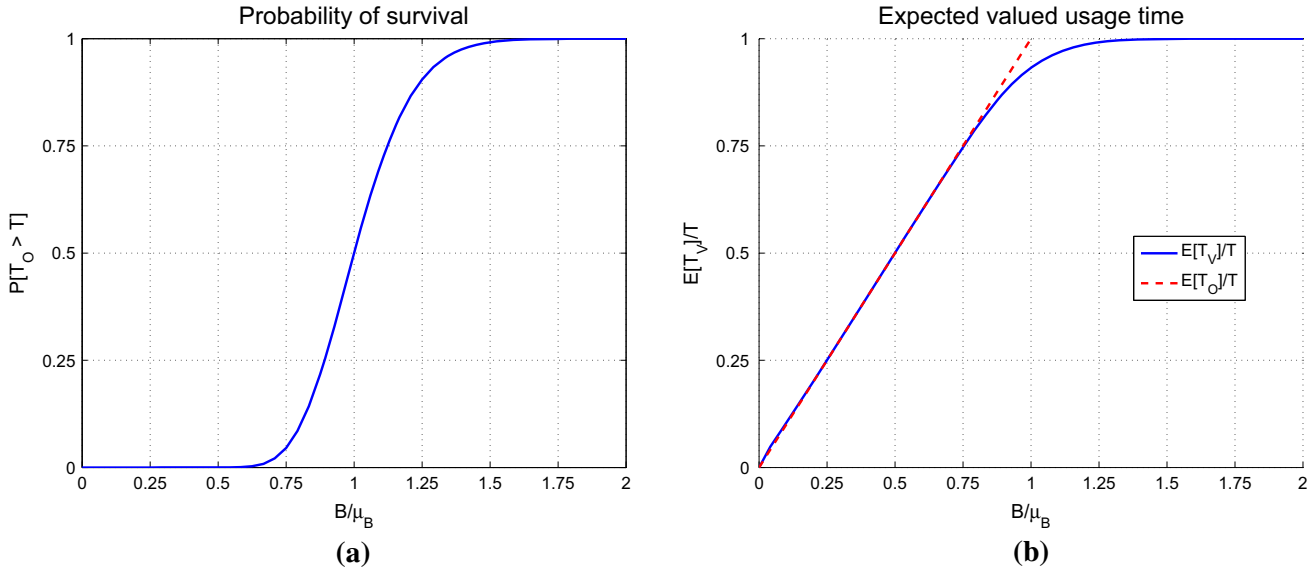

Fig. 6 Utility as functions of available battery for user categories C1 and C2. The target usage time T is fixed. $\mu_B = \lambda T/\nu$. **a** C1: probability of survival (18). **b** C2: expected valued usage time (21)

the full help requesting procedure. With this choice, (6) can be used to guide the design of cooperative rules.

According to (6), the rate of change of the helpee's utility with respect to battery must be greater than that of the helper. Since we have established that the battery consumption process under our model can be approximated as a Gaussian random process, we can use (18) and (21) to calculate the utility functions discussed in Sect. 3.1.4. We plot the values of those two functions with respect to the available battery in Fig. 6. Notice that we are looking at the resource dimension of the utility, as opposed to the time dimension as in Sect. 3.1.4.3.

In Fig. 6, the available battery B is normalized with respect to μ_B, the amount of battery that would give the expected time until outage $\mathbb{E}[T_O]$ equal to the target usage time T. From (50), we know that $\mathbb{E}[T_O] = B\nu/\lambda$. Therefore, $\mu_B = \lambda T/\nu$. In Fig. 6b, the dashed line represents the expected valued usage time when there is much less battery than required to meet target usage, as seen in (16). Since $\mathbb{E}[T_O]/T = B/\mu_B$, this line has slope 1.

We can see that for both utility functions, there exists a utility value above which the resource-slope decreases. Therefore we can use thresholding for our cooperative rules and design appropriate thresholds that guarantee beneficial cooperation. To achieve the condition in (6), we set a upper cooperative threshold (the helping threshold) γ_2 such that the helper is operating above this threshold, and thus on the slope-decreasing region. The helpee has to be operating below another threshold γ_1 ($\gamma_1 \leq \gamma_2$). For utility type 2, that is all we need to do to ensure that the helpee's resource-slope is greater than the helper's. For utility type 1, the helpee needs to be *above* $1-\gamma_2$ to have a steeper slope. The intuition is that if the helpee's available battery is so far off his target usage, a cooperative session will not improve his probability of survival much, and he is still very likely to go into outage. This is a characteristic of the all-or-nothing utility type.

3.2.5 Evolution of user utility over time

In this section we describe what happens to the utility of a user as time progresses. For the simplicity of the discussion, let us assume that the consumption parameter L does not change. In this case, there are only two factors affecting the user's utility: the remaining time until the target usage T and the amount of remaining battery B. Between data bursts, the amount of remaining battery stays the same. The user's utility thus increases as the time until target usage decreases. When the user has a new data burst, the battery drops suddenly, which also leads to a sudden drop in utility.

To illustrate these evolutions, we simulate a user with random data bursts and plot the values of the two utility functions over time for this user in Fig. 7. For this case, the two types of utility function follow a quite similar path, albeit on different scales. This user starts out with a 0.3 probability of meeting his target usage. His expected usage duration at the beginning is 0.91 of his target usage duration T. There is a big data burst at $t = 0.05T$, resulting in a large dip in the user's utility. As time progresses from $t = 0.05T$ to $0.5T$, the user has less data than expected, thus his utility increases (on average). From $t = 0.5T$ to $0.7T$, the user uses the typical amount of data. His utility stays constant on average over this range. From $t = 0.7T$ to $0.8T$ he uses more data than expected, which results in a dip in utility values. His usage decreases to less than typical from $t = 0.8T$ to the target

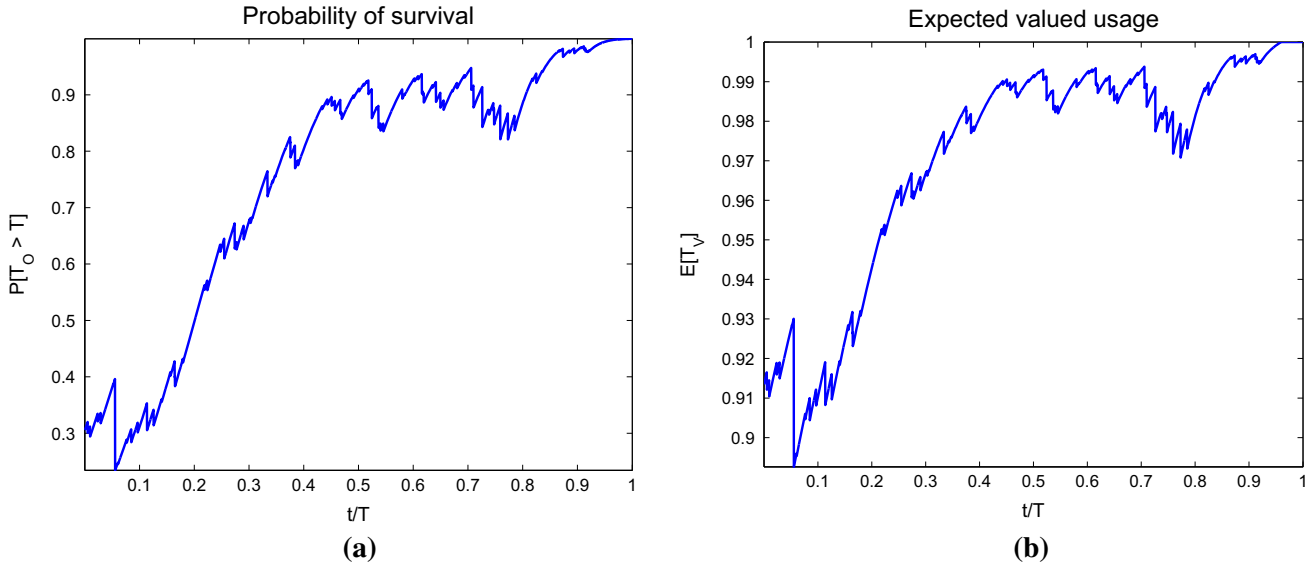

Fig. 7 Evolutions of user's utility. Notice the scale difference. **a** Utility for user category C1: probability of survival. **b** Utility for user category C2: expected valued usage time

usage T. He ends up meeting his target usage. However, he becomes relatively certain about that fact only at $t = 0.95T$.

4 User incentive

As we discussed in Sect. 1, the helpers do not get any immediate benefit from a cooperative BDS session. Therefore they need to be incentivized. A currency system is most suitable for BDS because we can leverage the centralized infrastructure. We discussed two such currency systems: virtual currency (token-based) and real currency.

The advantage of a virtual currency system is that it is self-contained. The amount of credits in the system is controlled by the network. Therefore the behavior of the users is predictable (as long as they are rational). The advantage of a real currency system is that it can potentially provide more cooperation as the users can always request for BDS service. However user interaction is required and the behavior is harder to predict.

4.1 Virtual currency

In a token-based incentive system, each user is initialized with a number of tokens, k_0, when they activate their phone number. To request BDS service, the user has to pay one token. The selected helper receives that token. Since the number of tokens of each user is kept by the network, fake tokens are not an issue. The network also sees data connections. Therefore a helper cannot lie that he relayed the helpee's traffic while he did not. Security of the token system therefore is not a major concern because of the centralized nature of BDS.

When a UE with k tokens receives `RRCConnReconfig` for BDS listeners (Fig. 1), it estimates the utility cost c for helping in a cooperative session. If the cost is less than the utility gain then the UE listens for `BDSDiscovery`. Let the value of k tokens be V_k. The UE listens for `BDSDiscovery` if $V_{k+1} - V_k > c$. [41] studies a token system for downlink relay service with the goal of improving data rates. It is shown that the optimal strategy for users is thresholding. A user receiving help request accepts if his number of tokens is smaller than a threshold, $k \leq K(c)$. If all users follow this optimal strategy, the network designer can control the total number of tokens in the network to achieve the maximum efficiency, i.e. the probability of a BDS request being accepted.

4.2 Real currency

We envision a real auction system where the helpee set a maximum amount of dollars that he is willing to pay for a help session, $d_{\max}$. This information is sent with `BDSInitSerReq`. Each potential helper sends an amount they want to receive for the service, d_i, in `BDSReply`. If there are more than one helpers whose request fees are less than $d_{\max}$, the AppSer selects the helper with the lowest request fee, and pays him the amount equal to the second lowest fee. This is known in the literature as a reversed auction. It is proven that the second lowest request fee is a form of Vickrey-Clarke-Groves (VCG) payment [42], and it achieves the optimal social outcome of everybody telling their true price.

Table 2 Simulation parameters

Parameter	Value
Cell radius	300 m
Number of UEs	500
Mean data inter-arrival time	30 s
Mean burst size	7800 bytes
Speed	0.1–6 m/s
Pause duration	0–300 s
Walk duration	30–300 s
Path loss compensation factor α	0.8
Constant energy cost factor	15 mJ
Base power P_0	−69 dBm
Maximum transmit power	24 dBm
Modulation order	QAM16
Code rate	1/3
Carrier frequency	2 GHz
eNodeB antenna height	25 m
UE antenna height	1.5 m
Number of walls for indoor NLOS	1
Cooperation threshold γ_1, γ_2	0.5, 0.9
Cooperation path loss threshold	110 dB
Cooperation radius	30 m

A real currency system is simple to implement. However, user interaction is expected to prevent "surprised" large phone bills. In crowded area (e.g. malls), there are plenty of potential helpers (high supply). Therefore the service will be cheaper. In remote area (e.g. parks), there are fewer potential helpers (low supply). As a result the service will be more expensive. The users, with some level of software automation, have to adjust their prices based on the area. We foresee a tendency that the users will keep their battery high in order to gain money. This change of behavior is interesting to study, but it is out of the scope of this paper.

5 Performance analysis

We established in Sect. 3.2 that by using thresholding, we can ensure that the cooperative sessions in BDS improve the overall network performance. In this section, we analyze this performance improvement through simulation. Our simulation setup is described in [14]. In particular, we use 3GPP reports [37,38,43] to set the parameters of our traffic model. We use WINNER II channel models [16] for our communication links. We use urban macro-cell model (scenario C2) for UE-eNodeB links and indoor office model (scenario A1) for UE-UE links. We use a modified version of the random waypoint model to simulate user mobility. The reception and idle circuit energy consumption is modeled as a constant factor, the value of which is derived from [37]. In this work, we implement new functionalities to calculate battery utility to use in cooperative decisions. The simulation parameters are shown in Table 2. Our simulator source code is available at [18].

We compare the performance of the UEs when they do and do not cooperate. When cooperation is used, we compare the cooperative rules using probability of survival $u_1(\cdot)$ (category C1—Sect. 3.1.4), expected valued usage time $u_2(\cdot)$ (category C2), and battery level B (used in [14]) as thresholds. The valued usage time as a fraction of the target usage time, T_V/T, of the UEs for those algorithms are shown in Fig. 8. The probability of survival for all 4 algorithms can

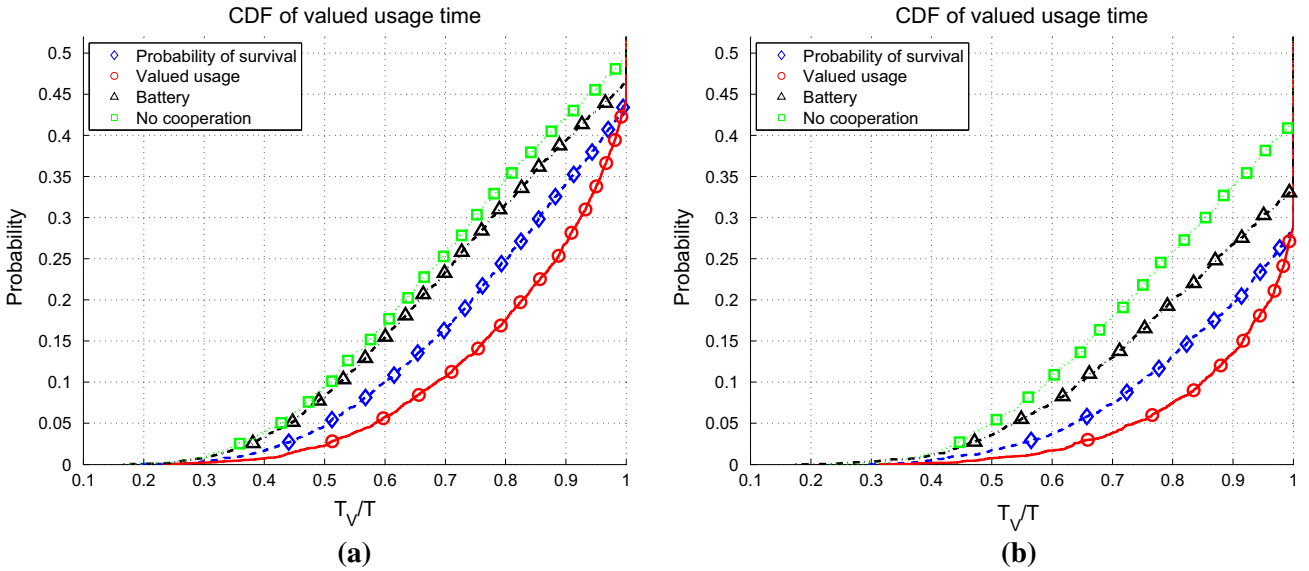

Fig. 8 Cumulative distribution functions of the valued usage time for 3 cooperative algorithms and no cooperation. The higher battery capacity is 14 % more than the lower battery capacity. **a** Lower battery capacity. **b** Higher battery capacity

Table 3 Overall network gains in valued usage time

	$u_1(\cdot) = \mathbb{P}[T_O > T]$ (%)	$u_2(\cdot) = \mathbb{E}[T_V]/T$ (%)	B (%)
Lower battery capacity	7	11	2
Higher battery capacity	7	10	1

Table 4 Overall network gains in probability of survival

	$u_1(\cdot) = \mathbb{P}[T_O > T]$ (%)	$u_2(\cdot) = \mathbb{E}[T_V]/T$ (%)	B (%)
Lower battery capacity	6	6	4
Higher battery capacity	13	13	8

also be inferred from Fig. 8. The intersecting points of the curves with the right-most vertical line, $T_V/T = 1$, are the probabilities of outage. In addition, we study the level of cooperation, which leads to performance gain, as the amount of resource in the network changes. In Fig. 8a, the users have low battery capacity, resulting in a probability of outage of 0.5. In Fig. 8b, we increase the battery capacity of the users by 14%, which results in a lower probability of outage of 0.41. We show the overall network gains in valued usage time as a percentage in Table 3. The overall gains in probability of survival are shown in Table 4.

We can clearly see that cooperation provides benefit over no cooperation. We also see that using utility functions as thresholds is better than using battery level. As we discussed in Sect. 1, by factoring in the target usage, we can take advantage of more cooperative opportunities than considering the battery level alone. Between the two utility functions, $u_2(\cdot)$ performs better when we consider valued usage time. This is consistent because it is designed for this performance metric. Interestingly, it can be seen that $u_2(\cdot)$ does not have any significant performance loss compared to $u_1(\cdot)$ for category C1. Therefore we can conclude that the cooperative thresholds perform well in limiting the impact on the helpers.

We can see from Table 3 that the overall network gains in valued usage time (as a ratio) are similar for lower and higher battery capacity cases. However the helpees in the latter clearly benefit more, as can be seen from their CDF curves. This is because when the overall network resource increases, there are more helpers and fewer helpees. As a result, each helpee receives a higher benefit. In addition, the fraction of helpees brought out of outage also becomes more significant. This leads to a larger increase in probability of survival, as evident from Table 4.

We further quantify the level of cooperation by studying the probabilities that a BDS request is accepted in the 2 cases of varying battery capacity. These probabilities are shown in Table 5. We can see that using utility functions creates at least twice the amount of cooperation compared to using

Table 5 Probability that a BDS request is accepted

	$u_1(\cdot) = \mathbb{P}[T_O > T]$	$u_2(\cdot) = \mathbb{E}[T_V]/T$	B
Lower battery capacity	0.46	0.57	0.25
Higher battery capacity	0.51	0.65	0.27

battery level B. In addition, $u_2(\cdot)$ consistently leads to more cooperation than $u_1(\cdot)$. This explains the larger amount of valued usage time created by using $u_2(\cdot)$. It is also clear that there are more chances for cooperation to take place when the network resource is high.

6 Conclusions

In this paper we have shown that we can prolong the battery life of mobile devices by utilizing diversity of usage in cellular networks. In particular, we developed a Proximity Service (ProSe) for future LTE networks which allows UEs to cooperatively relay traffic of one another. We named our system the "Battery Deposit Service" (BDS). To utilize diversity of usage, we must understand the value of battery for the UEs. We proposed a general framework to study utility of a resource. We applied this framework to BDS and showed that by setting appropriate thresholds as cooperative rules, the performance of the network is guaranteed to improve. It is important to provide incentive for users to cooperate. We discuss currency systems using virtual tokens and real money to incentivize users.

We believe that diversity of usage is an important concept and warrants further study. In particular, combining diversity of usage with traditional types of diversity (time, frequency, space) could yield more realistic results. Applying our framework for studying utility to other systems is also an interesting research direction. In particular, for BDS, we do not need to consider the transfer graph. This graph can be significant in the design of other systems.

Acknowledgments This material is based upon research partially supported by the National Science Foundation (NSF) grants CNS1018 346 and CNS1035655.

Appendices

Proof of Lemma 1

Since the consumption process $\zeta_L(\cdot)$ is non-negative, and the utility function is monotonically non-decreasing in B, the helper will never gain utility after a cooperative session

$$u_j(B_j - \zeta_{L_j}(T_c), T_j - T_c, L_j) - u_j(B_j - \zeta_{L_j}(T_c) - \Delta B_{ji}, T_j - T_c, L_j) \geq 0. \quad (57)$$

From (4)

$$u_i(B_i - \zeta_{L_i}(T_c) + \Delta B_{ji} - \delta_{ji}, T_i - T_c, L_i) - u_i(B_i - \zeta_{L_i}(T_c), T_i - T_c, L_i) \geq 0. \quad (58)$$

(5) follows from property (1) of the utility function. □

Expected valued usage time for Gaussian consumption process

We want to calculate the expected valued usage time $\mathbb{E}[T_V]$ for the case the consumption process $\zeta_L(t)$ is Gaussian. As seen in (20), the time until outage T_O is approximated as a Gaussian random variable $\mathcal{N}(\mu, \sigma^2)$. From (10)

$$\begin{aligned}\mathbb{E}[T_V] &= T - \int_0^T (T-\tau)\frac{1}{\sqrt{2\pi\sigma^2}} e^{-\frac{(\tau-\mu)^2}{2\sigma^2}} d\tau \\ &= T - (T-\mu)\int_0^T \frac{1}{\sqrt{2\pi\sigma^2}} e^{-\frac{(\tau-\mu)^2}{2\sigma^2}} d\tau \\ &\quad + \int_0^T (\tau-\mu)\frac{1}{\sqrt{2\pi\sigma^2}} e^{-\frac{(\tau-\mu)^2}{2\sigma^2}} d\tau. \end{aligned} \quad (59)$$

Since $T_O \geq 0$, for the approximation $T_O \sim \mathcal{N}(\mu, \sigma)$ to hold we need $\Phi(\frac{-\mu}{\sigma}) \approx 0$. This is true for sufficiently large μ. Consequently, we have

$$(T-\mu)\int_0^T \frac{1}{\sqrt{2\pi\sigma^2}} e^{-\frac{(\tau-\mu)^2}{2\sigma^2}} d\tau \approx (T-\mu)\Phi\left(\frac{T-\mu}{\sigma}\right). \quad (60)$$

To compute the last term of (59), we make the change of variable $u = \frac{(\tau-\mu)^2}{2\sigma^2}$. We have $(\tau-\mu)d\tau = \sigma^2 du$. Therefore,

$$\begin{aligned}&\int_0^T (\tau-\mu)\frac{1}{\sqrt{2\pi\sigma^2}} e^{-\frac{(\tau-\mu)^2}{2\sigma^2}} d\tau \\ &= \int_{\frac{\mu^2}{2\sigma^2}}^{\frac{(T-\mu)^2}{2\sigma^2}} \frac{\sigma}{\sqrt{2\pi}} e^{-u} du \\ &= \frac{\sigma}{\sqrt{2\pi}}\left(e^{-\frac{\mu^2}{2\sigma^2}} - e^{-\frac{(T-\mu)^2}{2\sigma^2}}\right). \end{aligned} \quad (61)$$

Finally (59) becomes

$$\begin{aligned}\mathbb{E}[T_V] &= T - (T-\mu)\Phi\left(\frac{T-\mu}{\sigma}\right) \\ &\quad + \frac{\sigma}{\sqrt{2\pi}}\left(e^{-\frac{\mu^2}{2\sigma^2}} - e^{-\frac{(T-\mu)^2}{2\sigma^2}}\right). \end{aligned} \quad (62)$$

References

1. Arthur, C. (2011). How the smartphone is killing the PC. http://www.guardian.co.uk/technology/2011/jun/05/smartphones-killing-pc. Accessed 15 Sept 2014.
2. Cisco. (2014). Global mobile data traffic forecast update, 2013–2018. http://www.cisco.com/c/en/us/sol-utions/collateral/service-provider/visual-networking-index-vni/white_paper_c11-520862.html. Accessed 15 Sept 2014.
3. Carroll, A., & Heiser, G. (2010) An analysis of power consumption in a smartphone. In *Proceedings of the 2010 USENIX conference on USENIX annual technical conference,USENIXATC'10* (p. 21). Berkeley, CA: USENIX Association.
4. Huang, J., Qian, F., Gerber, A., Mao, Z. M., Sen, S., & Spatscheck, O. (2012). A close examination of performance and power characteristics of 4G LTE networks. In *Proceedings of the 10th international conference on Mobile systems, applications, and services, MobiSys '12* (pp. 225–238). New York: ACM.
5. Badic, B., O'Farrrell, T., Loskot, P., & He, J. (2009). Energy efficient radio access architectures for green radio: Large versus small cell size deployment. In *IEEE 70th Vehicular Technology Conference Fall (VTC 2009-Fall)* (pp. 1–5).
6. Zhang, J., Ge, X., Chen, M., Jo, M., Yang, X., Du, Q., et al. (2013). Uplink energy efficiency analysis for two-tier cellular access networks using kernel function. *Telecommunication Systems*, *52*(2), 1305–1312.
7. Chiasserini, C.-F., & Magli, E. (2004). Energy-efficient coding and error control for wireless video-surveillance networks. *Telecommunication Systems*, *26*(2–4), 369–387.
8. Zhang, Y., Huang, L., Xu, H., & Yang, Z. (2013). An incentive energy-efficient routing for data gathering in wireless cooperative networks. *Telecommunication Systems*, *52*(4), 1977–1987.
9. Meshkati, F., Poor, H., Schwartz, S., & Balan, R. (2009). Energy-efficient resource allocation in wireless networks with quality-of-service constraints. *IEEE Transactions on Communications*, *57*(11), 3406–3414.
10. Ba, P., Niang, I., & Gueye, B. (2014). An optimized and power savings protocol for mobility energy-aware in wireless sensor networks. *Telecommunication Systems*, *55*(2), 271–280.
11. Miao, G., Himayat, N., & Li, G. (2010). Energy-efficient link adaptation in frequency-selective channels. *IEEE Transactions on Communications*, *58*(2), 545–554.
12. Hussain, S., Azim, A., & Park, J. (2009). Energy efficient virtual mimo communication for wireless sensor networks. *Telecommunication Systems*, *42*(1–2), 139–149.
13. Garnica, J., Chinga, R., & Lin, J. (2013). Wireless power transmission: From far field to near field. *Proceedings of the IEEE*, *101*(6), 1321–1331.
14. Ta, T., Baras, J. S., & Zhu, C. (2014). Improving Smartphone Battery Life Utilizing Device-to-device Cooperative Relays Underlaying LTE Networks. In *IEEE International Conference on Communications*.
15. Chon, Y., Ryu, W., & Cha, H. (2013). Predicting smartphone battery usage using cell tower id monitoring. *Pervasive and Mobile Computing*. http://www.sciencedirect.com/science/article/pii/S1574119213000801. Accessed 15 Sept 2014.
16. Kyosti, P., Meinila, J., Jamsa, T., Zhao, X., Hentila, L., Yli-talo, J., & Alatossava, M. (2007). WINNER II Channel Models. https://www.ist-winner.org/WINNER2-Deliverables/D1.1.2v1.1.pdf. Accessed 15 Sept 2014.
17. 3GPP. (1998). Selection procedures for the choice of radio transmission technologies of the UMTS, 3GPP Std. TR 30.03U.
18. Ta, T. (2014). Battery deposit service simulator. https://github.com/tuan-ta/bds. Accessed 15 Sept 2014.

19. Antonopoulos, A., Kartsakli, E., & Verikoukis, C. (2014). Game theoretic D2D content dissemination in 4G cellular networks. *IEEE Communications Magazine*, *52*(6), 125–132.
20. Antonopoulos, A., & Verikoukis, C. (2014). Multi-player game theoretic mac strategies for energy efficient data dissemination. *IEEE Transactions on Wireless Communications*, *13*(2), 592–603.
21. Janis, P., Yu, C.-H., Doppler, K., Ribeiro, C., Wijting, C., & Hugl, K. (2009). Device-to-device communication underlaying cellular communications systems. *International Journal of Communications, Network and System Sciences*, *2*(3), 169–178.
22. Yu, C.-H., Doppler, K., Ribeiro, C., & Tirkkonen, O. (2011). Resource sharing optimization for device-to-device communication underlaying cellular networks. *IEEE Transactions on Wireless Communications*, *10*(8), 2752–2763.
23. Elkotby, H., Elsayed, K., & Ismail, M. (2012). Exploiting interference alignment for sum rate enhancement in D2D-enabled cellular networks. In *Proceedings of IEEE WCNC 2012*.
24. Kone, V., Yang, L., Yang, X., Zhao, B.Y., Zheng, H. (2010). On the feasibility of effective opportunistic spectrum access. In *Proceedings of the 10th annual conference on Internet measurement, IMC '10* (pp. 151–164). NewYork, NY: ACM
25. 3GPP. (2013). Technical Specification Group Services and System Aspects; Feasibility study for Proximity Services (ProSe) (version 12.1.0), 3GPP Std. TR 22.803.
26. Raghothaman, B., Deng, E., Pragada, R., Sternberg, G., Deng, T., & Vanganuru, K. (2013). Architecture and protocols for LTE-based device to device communication. In *International Conference on Computing, Networking and Communications (ICNC)* (pp. 895–899).
27. Yang, M. J., Lim, S. Y., Park, H. J., & Park, N. H. (2013). Solving the data overload: Device-to-device bearer control architecture for cellular data offloading. *IEEE Vehicular Technology Magazine*, *8*(1), 31–39.
28. Kansal, A., Hsu, J., Zahedi, S., & Srivastava, M. B. (2007). Power management in energy harvesting sensor networks. *ACM Transactions on Embedded Computing Systems*, *6*(4), 32.
29. Buttyan, L., & Hubaux, J.-P. (2001). Nuglets: A virtual currency to stimulate cooperation in self-organized mobile ad hoc networks. Technical Report.
30. Anderegg, L., & Eidenbenz, S. (2003). Ad hoc-vcg: a truthful and cost-efficient routing protocol for mobile ad hoc networks with selfish agents. In *Proceedings of the 9th annual international conference on Mobile computing and networking, MobiCom '03* (pp. 245–259). NewYork, NY: ACM
31. Chen, B. B., & Chan, M. C. (2010). Mobicent: a credit-based incentive system for disruption tolerant network. In *INFOCOM, Proceedings IEEE, March 2010* (pp. 1–9).
32. Duan, L., Kubo, T., Sugiyama, K., Huang, J., Hasegawa, T., & Walrand, J. (2012). Incentive mechanisms for smartphone collaboration in data acquisition and distributed computing. In *INFOCOM, Proceedings IEEE, March 2012* (pp. 1701–1709).
33. Nakamoto, S. (2009). Bitcoin: A peer-to-peer electronic cash system. http://bitcoin.org/bitcoin.pdf. Accessed 15 Sept 2014.
34. Wei, K., Smith, A., Chen, Y.-F., & Vo, B. (2006). Whopay: A scalable and anonymous payment system for peer-to-peer environments. In *26th IEEE International Conference on Distributed Computing Systems. ICDCS 2006* (p. 13).
35. Baker, M. (2011). Chapter 18. *Uplink Transmission Procedures* (pp. 449–462). New York: Wiley.
36. 3GPP. (2011). Evolved Universal Terrestrial Radio Access (E-UTRA); Physical layer procedures (version 10.4.0), 3GPP Std. TS 36.213.
37. Nokia Corporation (2012). Further results on network signalling load and UE power consumption (R2–120367). Nokia Corporation.
38. Renesas Mobile Europe Ltd. (2012) Impact of DRX to always-on background traffic (R2–120578). Renesas Mobile Europe Ltd.
39. NIST. (2014). Incomplete beta functions. http://dlmf.nist.gov/8.17. Accessed 15 Sept 2014.
40. Bremaud, P. (1999). *Markov chains, Gibbs fields, Monte Carlo simulations, and queues*. Berlin: Springer.
41. Xu, J., & van der Schaar, M. (2013). Token system design for autonomic wireless relay networks. *IEEE Transactions on Communications*, *61*(7), 2924–2935.
42. Nisan, N., Roughgarden, T., Tardos, E., & Vazirani, V. V. (2007). *Algorithmic Game Theory*. New York: Cambridge University Press.
43. 3GPP. (2012). LTE Radio Access Network (RAN) enhancements for diverse data applications, 3GPP Std. TR 36.822.

Tuan Ta is a Ph.D. candidate at the Electrical and Computer Engineering Department, University of Maryland College Park. He received his B.S. (High Honors) in Electrical and Computer Engineering from The University of Texas at Austin in 2009. He received the Clark School of Engineering Distinguished Fellowship in 2009. He was a 2014 University of Maryland Invention of the Year Finalist. His research interests include next generation wireless communication systems, and physical layer methods for security and privacy.

John S. Baras holds the Lockheed Martin endowed Chair in Systems Engineering, at the Institute for Systems Research (ISR) and Electrical and Computer Engineering Department, of the University of Maryland College Park, which he joined in 1973. A graduate of the National Technical University of Athens, Greece, he received the M.S., Ph.D. in Applied Mathematics from Harvard University in 1971, 1973. He is also currently on the faculty of the Applied Mathematics Program, of the Fischell Department of Bioengineering and of the Mechanical Engineering Department. He was the Founding Director of the ISR from 1985 to 1991. Since 1991, he has been the Founding Director of the Maryland Center for Hybrid Networks (HYNET). He is a Life Fellow of IEEE, a Fellow of SIAM, and a Foreign Member of the Royal Swedish Academy of Engineering Sciences. He received the 1980 George Axelby Prize from the IEEE Control Systems Society, the 2006 Leonard Abraham Prize from the IEEE Communications Society, the 2014 Tage Erlander Guest Professorship from the Swedish Research Council, and a 2014-2017 Hans Fischer Senior Fellowship from the Institute for Advanced Studies of the Technical University of Munich. Professor Baras' research interests include control, communication and computing systems.